https://doi.org/10.1016/j.jaerosci.2021.105802

Experimental study of particle deposition on patterned microstructured surfaces in a chamber environment

Xiaoling Zhong, Sau Chung Fu, Ka Chung Chan and Christopher Y.H. Chao*

Department of Mechanical Engineering,

The University of Hong Kong, Hong Kong, China

*Corresponding author: *scfu@hku.hk*

Address all correspondence to:

Sau Chung Fu

Department of Mechanical Engineering

The University of Hong Kong

Pokfulam,

Hong Kong, China

Email: scfu@hku.hk

Fax: (852) 2858-5415

Tel: (852) 3910-2154

Experimental study of particle deposition on patterned microstructured surfaces in a chamber environment

Xiaoling Zhong, Sau Chung Fu, Ka Chung Chan and Christopher Y.H. Chao*

Department of Mechanical Engineering,

The University of Hong Kong, Hong Kong, China

*Corresponding author: scfu@hku.hk

Abstract

Indoor respirable suspended particles may accumulate on textured surfaces such as sofa surfaces and office partitions via particle deposition. Previous studies mainly focus on particle deposition on non-patterned rough surfaces or patterned surfaces with texture scale larger than millimeters, and it is generally concluded that deposition rate increases due to the roughness. However, many indoor surfaces are patterned textures with scale in the order of 100 μm and there is a lack of study of particle deposition behavior in this regime. This study investigates the effect of patterned microstructured surfaces on particle deposition in a turbulent chamber. Different shapes (triangular, rectangular, semi-circular convex and semi-circular concave ribbed structures) and pitch-to-height ratios (i.e. ratio of spacing to height) of patterned structures were studied. Particle sizes ranging from 0.3 μm to 5 μm in diameter were tested. It is found that for submicron particles, deposition velocity was increased by the patterned microstructures, and triangular-ribbed surfaces achieved the highest deposition velocity, which

was 10 times higher than that on a non-patterned surface. For micron particles, it is found that deposition velocity was lower than that of a non-patterned surface. Our results show that particle deposition is not always enhanced by roughness and it is possible to be reduced by a suitable length scale of patterned structures.

Keywords

Indoor air quality, Particle deposition, Microstructured surface, Shape, Pitch-to-height ratio, Turbulence

1. Introduction

Indoor air pollution has been drawing increasing attention over the past few decades as a result of increasing concern about the effects of particle exposure on human health (Jones, 1999; Pope et al., 1991). The knowledge of particle deposition onto surfaces can contribute to the decrease in indoor airborne particle concentration, as well as exposures (Lai, 2002). Particle deposition in indoor environments or experimental chambers has been widely studied (Cheng, 1997; Lai et al., 2008; Lai, 2006; Thatcher and Nazaroff, 1997; Thatcher et al., 1996; Thatcher, et al., 2002; Xu et al., 1994; Yu et al., 2017), most of which focus on non-patterned surfaces with different roughness. Hussein et al. (2009) studied the deposition rate of aerosol particles (diameters between 0.03 and 5 μm) on rough surfaces like wallpapers, wall-plaster, and two types of carpets in a chamber environment. The deposition rate of the aerosol particles was affected by surface roughness, mixing intensity, and particle size. The highest deposition rate on those rough surfaces was up to 20 times as that on a smooth aluminum surface. Abadie et

al. (2001) also studied the effect of wall textures on particle deposition and they found that the deposition on rough wallpapers was more than that on smooth surfaces. Lai and Nazaroff (2005) studied the monodisperse particles deposition onto smooth and rough vertical chamber surfaces using sandpapers. They found that the deposition velocity increased moderately with increasing surface roughness. Shimada et al. (1987) found that for monodisperse particles of 0.01-0.2 μm in diameter, the deposition rate of particles onto the rough surface was enhanced, compared with that onto a smooth surface, and as the roughness increased, the deposition rate increased. The rough surfaces in their experiments were sandpapers with different roughness. All these studied surfaces were non-patterned surfaces with different roughness. However, many indoor decoration surfaces in modern office buildings have patterned textures, e.g. surfaces of some wallpapers, nylon decoration surfaces on the sofa and office partitions. Results obtained from the previously mentioned studies on non-patterned surfaces might not be fully applied to patterned surfaces.

Previous studies have found that a small obstruction on a surface will affect the deposition rate on the surface. By repeating the obstruction on the surface in a regular pattern, it becomes a patterned surface. The shape of the obstruction (repeating unit) and the pitch-to-height ratio of the pattern (defined as the ratio of the spacing between two successive repeating units to the height of the repeating unit) are two important factors affecting particle deposition on a patterned surface. Lai et al. (1999, 2001, 2002) investigated the effects of 2D and 3D square-shaped obstructions on particle deposition. It was found that the deposition velocity was

significantly increased due to these obstructions. Li et al. (1994) studied the deposition on surfaces with rectangular and trapezoidal obstructions. Their results indicated that the obstructions significantly enhanced particle deposition. The numerical study from Lu and Lu (2015a) also demonstrated that the particle deposition on various shapes of ribbed surfaces was different. They compared the deposition on squared, triangular and circular ribbed surfaces and found that the maximum deposition occurred on the squared ribbed surface. Another result from Lu and Lu (2015b) indicated that particle deposition enhancement increased with decreasing rib space. The maximum enhancement ratio reached to about 400 compared to a flat surface. Rashidi et al. (2017) also emphasized that the particle deposition could be enhanced with a larger pitch-to-height ratio of the two obstructions.

These studies successfully correlated the particle deposition with properties of the patterned surface, however, the scale of structures studied was in millimeter scale or larger, while many indoor decoration surfaces are in the scale of 500 μm or below, as shown in Figure 1. The influence of these smaller-scale patterned structures on particle deposition is unknown. Therefore, the objective of this research is to investigate the effect of microstructured surfaces in this length scale regime with different shapes and pitch-to-height ratios on particle deposition in chamber flow. This study can provide a better understanding of the role of microstructured surfaces on indoor particle deposition.

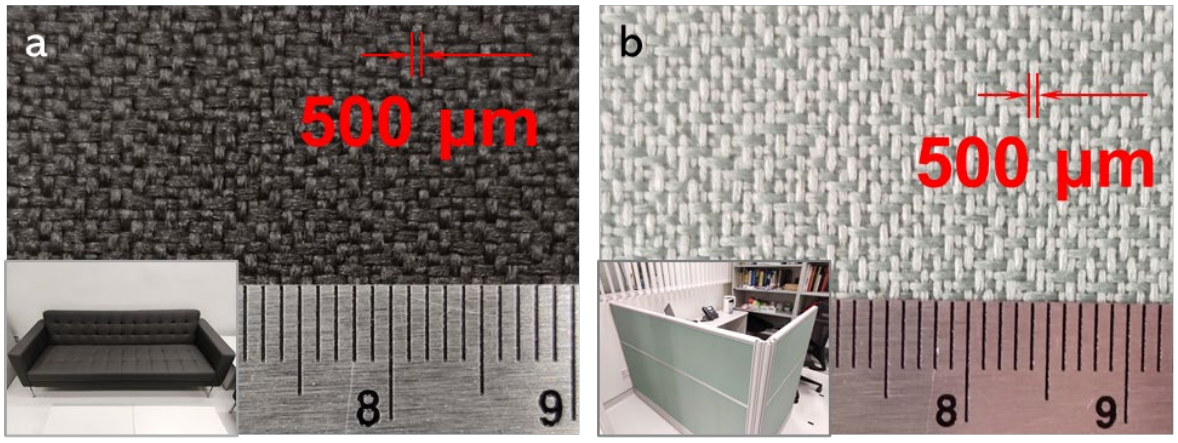

Figure 1 The surface structures on (a) office sofas and (b) partitions (b).

2. Methodology

2.1 Experimental setup

A small-scale chamber (300 mm × 300 mm × 300 mm) was fabricated by poly(methyl methacrylate) plates. A small boxer fan (SUNON, EE80252S1-0000-A99), suspended from the center of the chamber and blowing air towards the ceiling, was employed to mix the air inside. The experimental setup is illustrated in Figure 2. Before each experiment, the inner surfaces of the chamber and the fan were cleaned by acetone and ethanol, followed by an air flushing for about 3 minutes. Sample surfaces with different microstructures were put inside the chamber to investigate their effects on particle deposition. The samples surfaces were fabricated using a photopolymer material called VeroBlue by 3D printing on a substrate with the size of 250 × 250 × 0.5 mm (length × width × thickness). The surface roughness of our samples, including patterned and nonpatterned ones, was 1.65 μm, which was measured by a Veeco 3300 profiler. Four different microstructured ribs were investigated, including rectangular ribs, triangular ribs, semi-circular convex ribs and semi-circular concave ribs as shown in Figure 3. The height of

120 the rib was fixed as h = 500 μm. The width of the rib (i.e. the width of the base in the triangular
121 rib or the diameter of the semi-circular convex or semi-circular concave ribs) was $w = 2h$ = 1
122 mm. The pitch p is the separation distance between two successive microstructured ribs. For
123 each rib shape, at least 5 different ratios of the pitch to the height p/h were studied.
124
125 Particles were generated by particle generators and introduced into the test chamber. Two kinds
126 of aerosols were generated for testing, polydisperse particles and monodisperse particles. The
127 particle concentration inside the chamber was monitored by a particle counter. The
128 polydisperse particles were Arizona test dust with diameter ranges of 0-5 μm. A tailor-made
129 aerosol generator was designed and constructed to aerosolize the dust. It was a test bottle
130 containing a moderate amount of dust and connected with two tubes. One tube was connected
131 to the supply inlet of compressed air, which aerosolized the dust in the bottle, and the other
132 tube guided the aerosolized dust to the test chamber. The dust concentration in the test chamber
133 was monitored by an optical particle sizer (Model 3330, TSI, USA). The particles with
134 diameters from 0.3 to 5 μm were measured in the polydisperse experiment. The generation was
135 stopped when the particle concentration reached 3000 #/cm^3. Monodisperse particles were
136 generated by a condensation monodisperse aerosol generator (Model 3475, TSI, USA). In this
137 study, two particle sizes were tested, 0.4 μm and 2 μm in diameter. The material of the particle
138 was di-2-ethyl hexyl sebacate (DEHS). For the 2 μm particles, the measurement device was a
139 portable aerosol spectrometer (Model 1.108, Grimm, Germany), and a scanning mobility
140 particle sizer spectrometer (Model 3080, TSI, USA) was used to measure the 0.4 μm particles.

By using a concentration decay method, the deposition velocity due to the patterned surface can be determined by the continuously measured particle concentration. Measurement was stopped either when the concentration was less than 200#/cm^3 (for polydisperse particles), or the deposition process had lasted for 1 hour (for monodisperse particles). In both cases, the durations were long enough for an accurate decay method to be conducted. Each experiment was repeated at least 3 times.

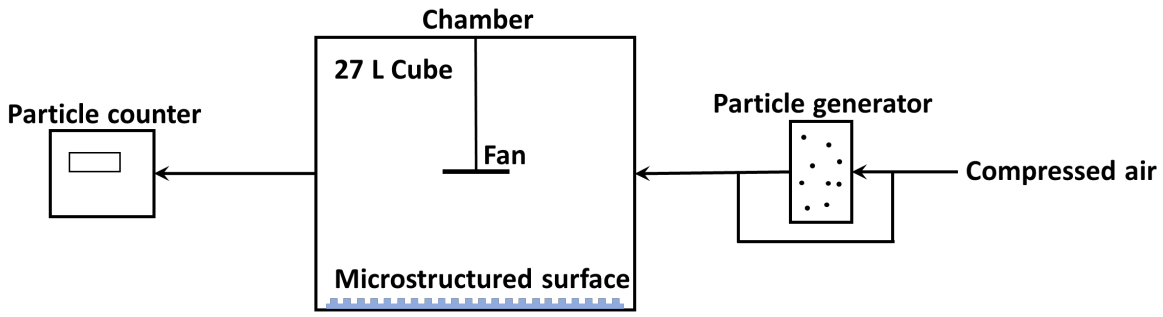

Figure 2 Schematic diagram of the experimental setup

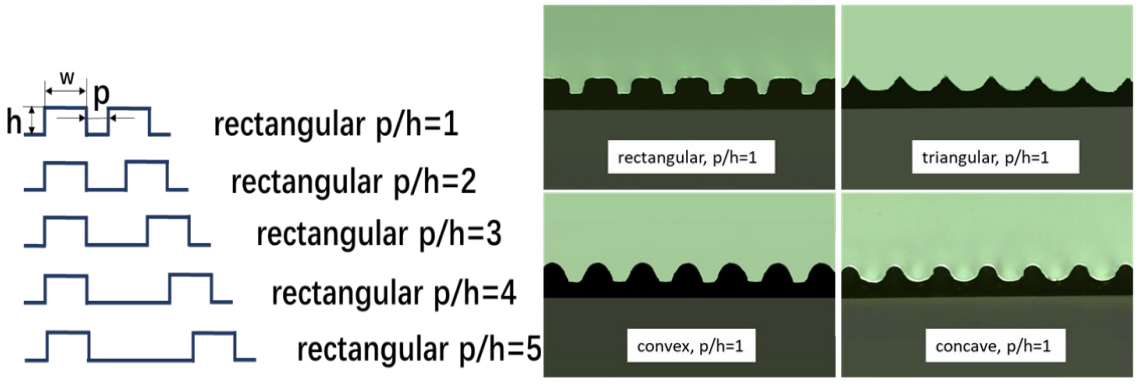

Figure 3 Schematic diagram for samples with rectangular shapes and photos for samples of all shapes with p/h=1.

2.2 Flow field measurement

In this study, the flow field in the middle plane of the chamber and a near-wall field on the chamber floor were measured by a particle image velocimetry (PIV) technique (LaVision, Germany). The tracer particles were olive oil in diameter smaller than 1 μm. The capturing frequency was 1 kHz. The setup is shown in Figure 4.

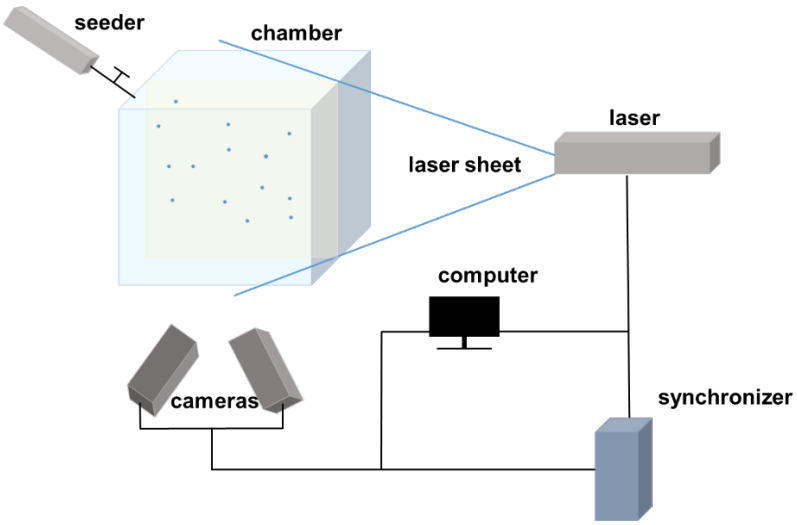

Figure 4 Schematic diagram of the PIV setup

2.3 Deposition effect calculated by decay method

For a well-mixed enclosed chamber with no particle generation, the particle concentration inside the chamber will decay with time and the governing equation can be expressed as

$$C(t) = C_0 e^{(-\lambda t)} \quad (1.)$$

where t is the time, C_0 is the initial particle number concentration (particle number per unit volume) and λ is the net particle decay rate with the dimension of 1/time. Thus, Eq. (1) can also be expressed as

$$\ln C(t) = -\lambda t + \ln C_0 \quad (2.)$$

and λ can be separated into two parts

$$\lambda = \lambda_{ilr} + \lambda_d \quad (3.)$$

where λ_{ilr} is the loss rate due to the instrumental sample flow rate, which is the instrumental sample flow rate divided by the chamber volume, and λ_d is the deposition rate. Based on the above model and the known parameters, the deposition rate λ_d could be calculated.

To better compare the effect of different microstructured surfaces, relative deposition rate, denoted as ε, was employed:

$$\varepsilon = \frac{deposition\ rate\ with\ a\ microstructured\ surface\ put\ inside\ the\ chamber}{deposition\ rate\ with\ a\ non-patterned\ surface\ put\ inside\ the\ chamber} \quad (4.)$$

The relative deposition rate is a dimensionless parameter and that of a non-patterned surface is equal to 1.

It should be noted that the deposition rate is a parameter to describe the overall deposition inside the chamber including all surfaces in the chamber, patterned or not. To study the deposition on a specific surface, deposition velocity is more useful. In the experiment of a patterned sample surface placing on the floor of the chamber, the relationship between the deposition rate of the chamber with a sample installed (λ_{ds}) and the deposition velocity on the sample surface (U_{dus}) can be described as

$$U_{dus} = \frac{\lambda_{ds}V - U_{dw0}A_w - U_{dd0}A_d - U_{du0}(A_u - A_s)}{A_s} \quad (5)$$

where A_w, A_d, A_u, A_s are the area of the four vertical walls, the area of the downward horizontal surface, the area of the upward horizontal surface, and the area of the patterned sample surface, respectively, U_{dw0}, U_{dd0} and U_{du0} are the deposition velocity of the vertical walls, the deposition velocity of the ceiling surface, and the deposition velocity of the floor area that was not covered by the patterned sample surface, respectively, and V is the volume of the chamber.

In the experiment without any sample surface inside, the relationship between the deposition rate (λ_{d0}) and the deposition velocities is

$$\lambda_{d0}V = U_{du0}A_u + U_{dw0}A_w + U_{dd0}A_d \quad (6)$$

The ratios of U_{du0}, U_{dw0} and U_{dd0} for monodisperse particles of 2 μm and 0.4 μm respectively will be obtained as described in section 2.4. By using the experimental result of λ_{d0} and substituting the ratio into Equation (6), the values of $U_{du0}, U_{dw0,}\ U_{dd0}$ can be obtained. Then the deposition velocity on the sample surface (U_{dus}) can be determined by Equation (5).

2.4 Deposition effect measured by microscope

Experiments were conducted to investigate the particle deposition on different orientations inside the chamber. In each experiment, three non-patterned samples were placed on the middle of the floor, wall and ceiling surface, respectively. The particles of 2 μm and 0.4 μm were tested respectively. Images before and after experiments were captured as shown in Figure 5(a) and further processed as shown in Figure 5(b). The black dots represent particles or defects. The total black area, and the whole image area were counted through the microscope. By subtracting the total black area before the experiment from those after the experiment, the deposition area was calculated. The deposition rate by the microscope was defined as

$$\xi = \frac{deposition\ area\ after\ experiments - deposition\ area\ before\ experiments}{investigated\ area} \quad (5.)$$

As shown in Figure 5(a), for 2 μm particles, after deposition for 1 h, it was clear that the deposition mainly occurred on the floor surface. The deposition rate by the microscope of 2

μm particle on the floor, wall and ceiling surface was 2.28%:0%:0.05%, which was essentially 1:0:0. Using the same method, the deposition rate by the microscope of 0.4 μm particles on the floor, wall and ceiling surface was essentially 1:1:1.

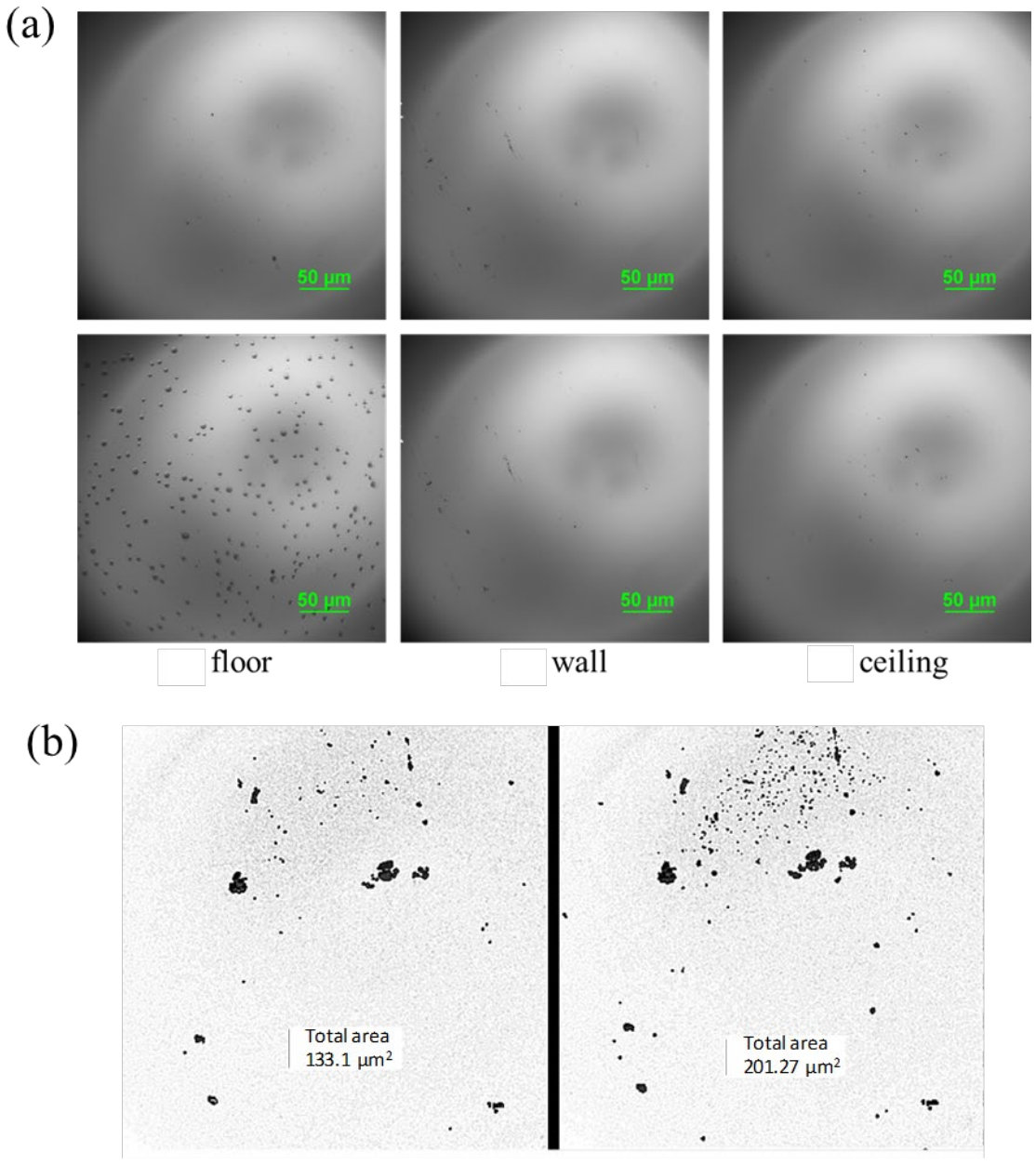

Figure 5 (a) Comparison of 2 μm particle deposition on different orientations before

experiments (top) and after experiments (bottom); (b) Processed images before experiments (left) and after experiments (right).

3. Results and discussion

3.1 Flow characteristics

The flow characteristic was investigated first because the particle deposition is affected by the flow. Two kinds of flow fields were measured: the middle plane of the whole chamber and a near-wall field at the bottom of the chamber immediately above the sample. For the whole chamber, two symmetric circulations were observed and illustrated as shown in Figure 6(a).

A near-wall flow field, as indicated by a yellow rectangle in Figure 6(a), was also investigated in detail. The mean vorticity contours in the near-wall flow field for two cases, with a microstructured surface and with a non-patterned surface, were compared in Figure 6(b). Stronger vorticity was produced on the bottom microstructured surface, compared to the non-patterned case. Besides, the enhanced vorticity showed a symmetrical distribution along the vertical centerline of the symmetric circulation flow. As shown in Figure 6(c), the turbulence kinetic energy (TKE) of the microstructured case was significantly higher than that of the non-patterned case, especially when the distance from the bottom surface was smaller than 5 mm. The enhanced TKE and vorticity are expected to affect the particle motions and shall be the reasons why the particle deposition was enhanced by the patterned surface as suggested in other studies (Lu and Lu, 2015c; Lu and Lu, 2016; Lu and Lu, 2017; Xu *et al.*, 2020; Xu *et al.*, 2020).

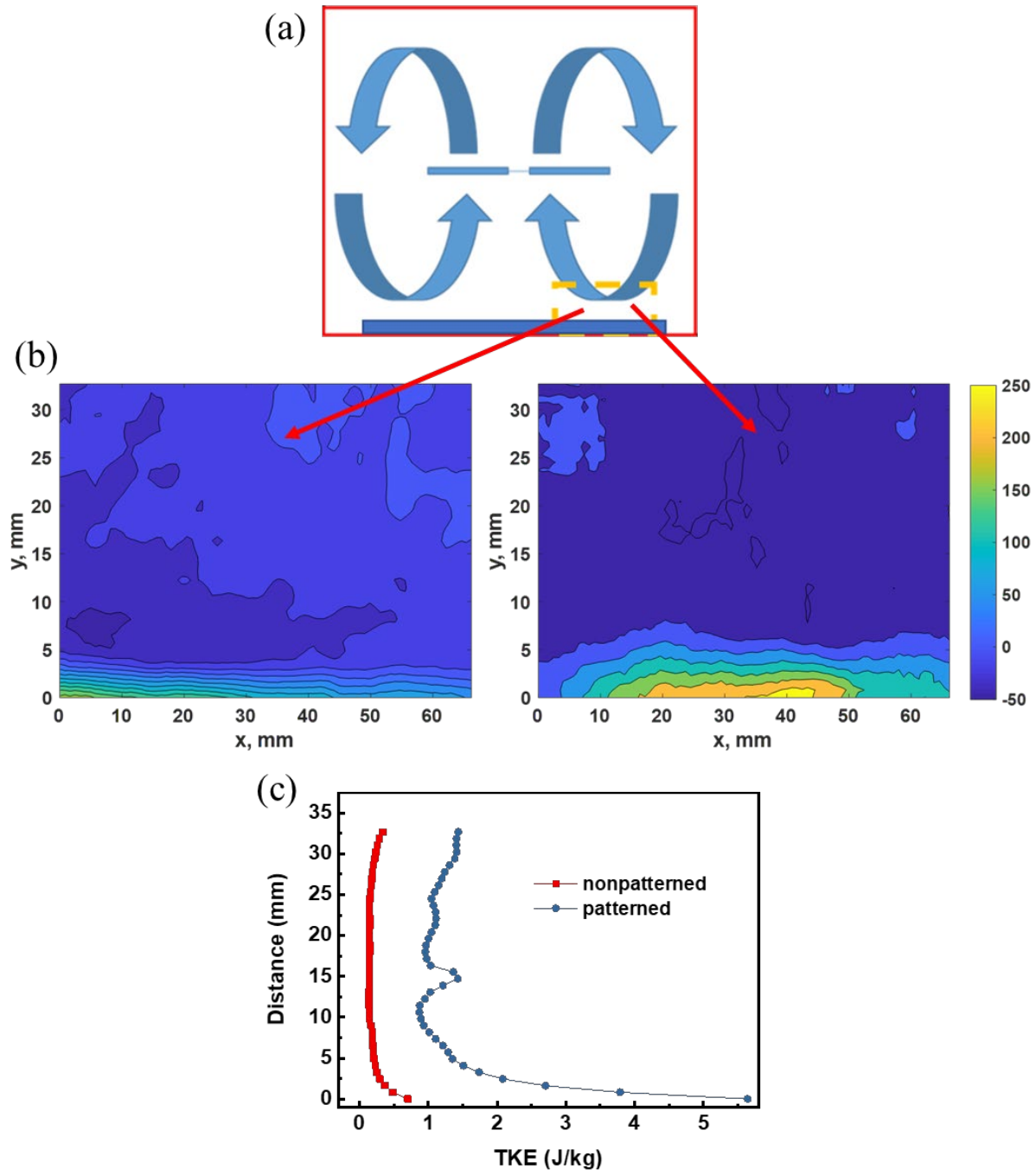

Figure 6 (a) Illustrative diagram of the flow condition in the middle plane; (b) Comparison of the vorticity on a non-patterned surface (left) and a patterned surface (semi-circular convex, p/h=1) (right); (c) Comparison of the turbulence kinetic energy in the near-wall field between the cases with a non-patterned surface and a microstructured surface. Y axis represents the distance between the investigation point and the bottom surface.

253

254 **3.2 Effect of microstructured surfaces on submicron particle deposition**

255 The results of how different pattern shapes affect submicron particle deposition are shown in
256 Figure 7. Polydisperse particles were used in the experiments. The relative deposition rate for
257 each shape was the average value of 5 samples with the same shape and different pitch-to-
258 height ratios (p/h = 1, 2, 3, 4 and 5). The relative deposition rates for all shapes were larger
259 than 1, which indicated that all microstructures enhanced submicron particle deposition,
260 compared with non-patterned surfaces. Among the investigated shapes, triangular
261 microstructures have the largest enhancement of deposition, followed by semi-circular convex,
262 rectangular, and concave microstructures. This indicated that the submicron particle deposition
263 rate on a surface was related to the shape of microstructures.

264

265 According to a numerical study carried out by Xu et al. (2020), the particle deposition of the
266 same four patterned shapes was investigated in a fully developed turbulent duct. They found
267 that all patterned shapes enhanced the particle deposition, while the enhancement of triangular
268 and semi-circular convex shapes was higher than that of the rectangular and concave
269 microstructures in a simulated duct flow. It should be noted that the pattern height in their
270 simulation was 2 mm, but the finding on the effect of shape was consistent with our
271 experimental results. The particle deposition mechanism was explained by the disturbance of
272 TKE at near-wall region and separation flow mechanism between two consecutive patterns.
273 Submicron particles followed the flow and were trapped into the cavity between two successive
274 ribs with the recirculation. However, the particles would not deposit on the surface, unless there

was a strong enough turbulent diffusion applied so that the submicron particles could diffuse through the near-wall boundary layers. There was a high-turbulence-kinetic-energy region at the top of the cavity, which is consistent with our experimental measurement, and this provided a suitable condition for submicron particles to deposit. The high-turbulence-kinetic-energy zone covered the whole cavity for the triangular shape, and only half of the cavity for the rectangular shape. This difference explained why the deposition of triangular microstructures was stronger than that of rectangular microstructures. It should be noted that a fully developed channel flow was studied by Xu et al. (2020), while a chamber flow, which is less unidirectional, was investigated in the current study. Therefore, the enhancement effect of a chamber flow is less significant than that of a channel flow.

The effect of *p/h* ratios on submicron particle deposition is shown in Figure 8. Monodisperse particles with 0.4 μm in diameter were used in the experiments. For 0.4 μm particles, deposition velocity decreased when *p/h* ratio increased. The magnitude of enhancement effect of microstructured surfaces decreased as the *p/h* ratio increased, until the *p/h* ratio was large enough and the effect eventually disappeared, compared with non-patterned surfaces.

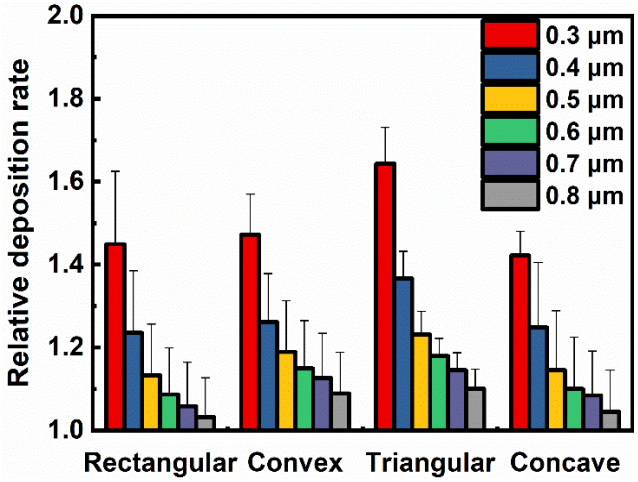

Figure 7 Comparison of relative deposition rates for different submicron particle sizes

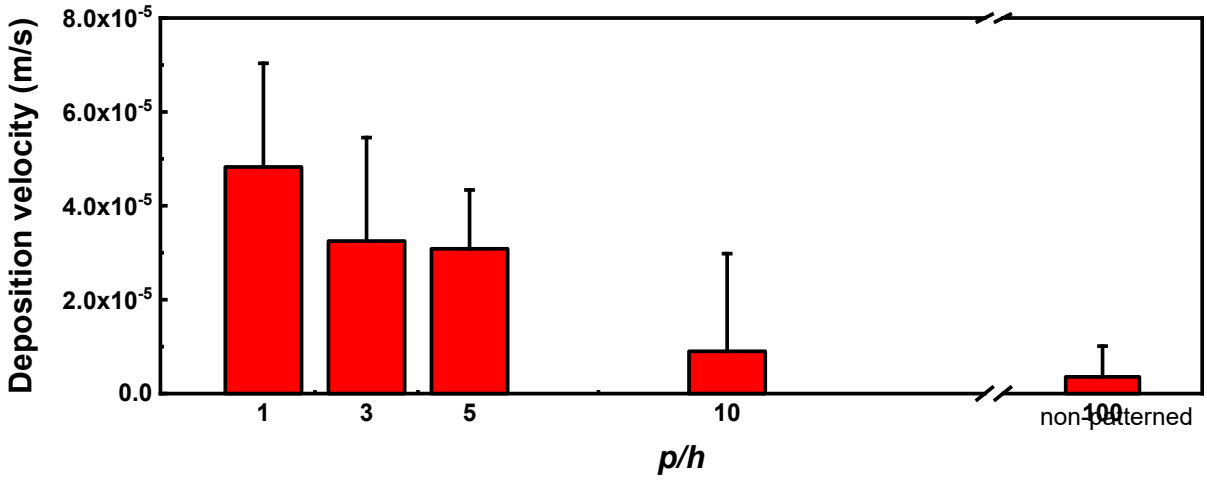

Figure 8 Comparison of deposition velocity of 0.4 μm particles for different *p/h* ratios

3.3 Effect of microstructured surfaces on micron particle deposition

The effect of shapes of microstructures on micron particle deposition is shown in Figure 9. Polydisperse particles were used in the experiments. The relative deposition rate was in the range of 0.79-1.07 in all cases. Unlike the cases of submicron particles, there was no obvious difference in the micron particle deposition rate for different microstructure shapes, and the variance of deposition rates for different shapes was within 3% (variance was calculated as the standard deviation divided by average relative deposition rate), which suggested that the

303 effect of microstructure shape on deposition rate was insignificant for micron particles.

304

305 The effect of *p/h* ratios on micron particles deposition is shown in Figure 10. Particles with a
306 highly monodisperse size of 2 μm were used in the experiments. Deposition velocity increased
307 with increasing *p/h* ratio, closing to the deposition velocity of the non-patterned surface. This
308 trend indicated that the microstructured surfaces have a reduction effect on micron particle
309 deposition, which was different from the cases of submicron particles. To further investigate
310 this reduction effect, the particle deposition on the cavity floor (i.e. the flat surface between
311 two successive microstructures) for different *p/h* ratios, was observed under a microscope. As
312 shown in Figure 11, for $p/h = 1$, there was no deposition on the cavity floor; for $p/h = 3$, and
313 $p/h = 10$, more particles were deposited on the cavity floor, while the deposition for $p/h = 10$
314 was as much as that of the non-patterned surface. The deposition distribution on the cavity
315 floor was also studied in Figure 12. Five locations on the cavity floor were observed under the
316 microscope. The deposition rate by microscope showed a centrally symmetric distribution; it
317 was nearly constant in the middle of the cavity floor, while at the corner sides it was lower,
318 where according to the simulation (Xu et al., 2020), separated shear flow occurred.

319

320 A similar observation was made by Wang et al. (2018), who investigated particle deposition
321 on textile surfaces and found a particular case that the deposition of 1.6 μm particles on textile
322 material decreased with the increase in surface roughness when the angular velocity of the
323 ceiling fan was the lowest in their experiments. Besides, in the experiments of Usui et al. (2004),

they investigated the effect of rib design on fouling from diesel particulate and found micron particle deposition on a semi-circular ribbed surface was reduced at a factor of 38% in the rib height of 500 μm, compared with a flat and smooth surface. While extending the rib height from 500 μm to 1 mm and 2 mm, the deposition was increased and for the largest riblets, they found micron particle deposition was enhanced up to about 9% compared with a flat and smooth surface. Concluded from their microscopic images, they attributed the reduction deposition effect to the minimal deposition onto the valley of the riblet. These findings are consistent with our experimental results.

In general, a rough surface, which generates more turbulent eddies, would enhance micron particle deposition significantly (Hussein et al., 2012). However, micron particle deposition on patterned micron structures is reduced as demonstrated by our experiments. Particles in micron-size (1-10 μm) fall into the eddy diffusion–impaction regime (Lai et al., 2002; Li et al., 1994) in which the turbulent eddies in the turbulent core and buffer layer induce enough inertia for particles to cross the viscous sublayer and deposit on the surface. As indicated by Hinds (1999), diffusion mechanism in micron-sized particles is not as important as in the submicron particles. It is suspected that the additional turbulent eddies generated by the microstructures in the setting of the current study are not strong enough for the micron particles to diffuse across the boundary layer. On the other hand, the recirculation at the upstream and downstream of the cavity prevent the particle from moving close to the wall surface. As observed in Figure 12, the vortexes, which prevented the particles from reaching the wall surface, were located at the

upstream and downstream of the cavity. Thus deposition cannot occur in the region covered by the vortices, and the area for particle deposition was reduced. Therefore the effective area for particle deposition is smaller and the deposition rate decreases when compared to a non-patterned surface.

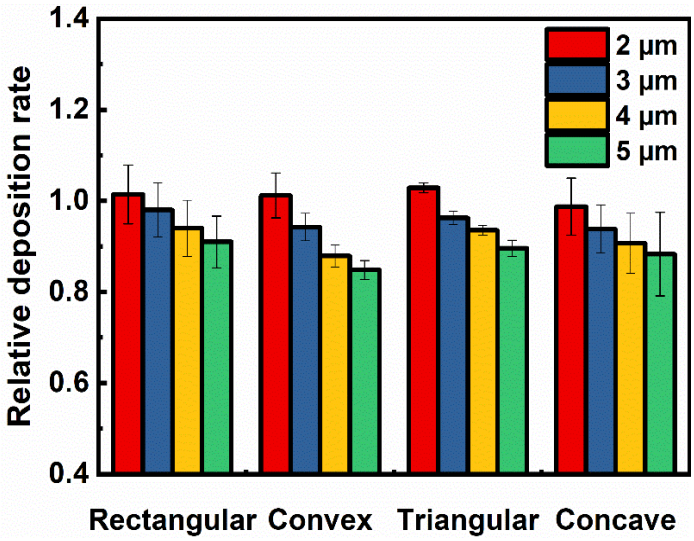

Figure 9 Comparison of relative deposition rate on different shapes, rectangular, semi-circular convex, triangular, semi-circular concave, for micron particles

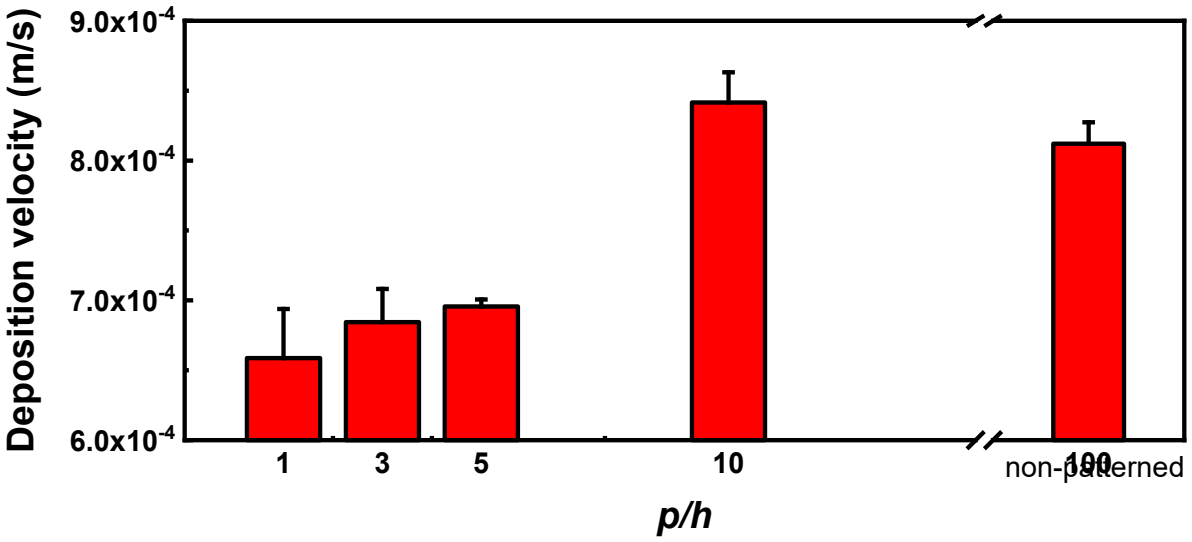

355

356 Figure 10 Comparison of deposition velocity of 2 μm particles for different *p/h* ratios

357

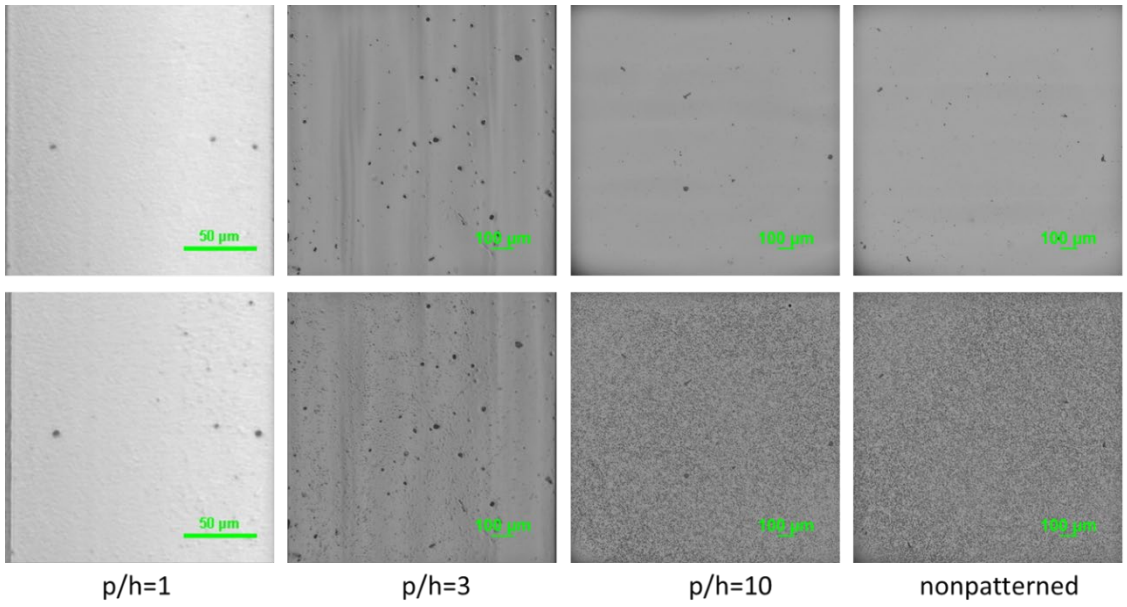

358

359 Figure 11 Comparison of 2 μm particle deposition effect for different *p/h* ratios on the cavity

360 floor before experiments (top) and after experiments (bottom)

361

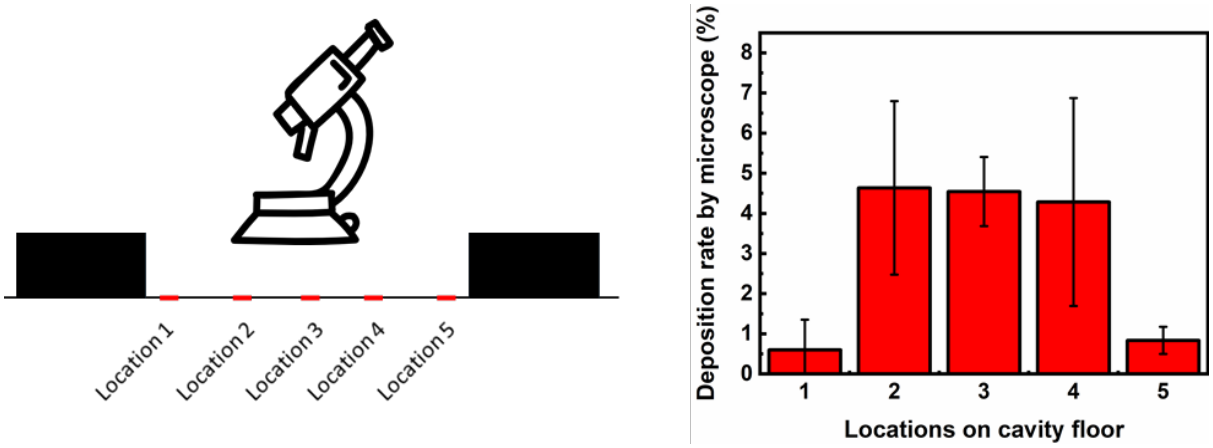

362

363 Figure 12 Deposition rate by microscope of 2 μm particles on different locations on the

364 cavity floor for the patterned surface of rectangular, p/h=5

365

366 **3.4 The influence of microstructured surfaces on indoor particle concentration**

367

368 In determining exposures to indoor particles, the particle concentration of a room is commonly

369 modeled by a well-mixed mass-balance equation (e.g. Abadie et al., 2001; Lai, 2002; Thatcher

370 et al., 2002), in which the deposition loss rate due to indoor surfaces is an essential parameter.

371 Since patterned texture surfaces are common in modern indoor environments, it is important

372 to consider the effect of micropatterns on the disposition loss rate. A comparison between a

373 hypothetical room with microstructured surfaces (rectangular shape and p/h=1) and a control

374 room with smooth surfaces was conducted and the result is shown in Table 1. The two rooms

375 are denoted as “patterned room” and “control room” respectively. The room sizes were the

376 same as 10 m^2 in area, and 2.5 m in height, as a normal living room size in Hong Kong (Lee et

377 al., 2002). The initial particle number concentration, C_0, was assumed to be 2×10^{11} #/m^3, which

378 was the particle concentration in a living room during cooking (Wan et al., 2011). The ratio of

379 particle concentration in the patterned room to that of the concentration in the control room, γ,
380 was calculated by the mass-balance equation. It was found that the submicron particle
381 concentration in the patterned room was 70% of that in the control room after 1-hour deposition,
382 and only 0.02% of that in the control room after deposition for 1 day, which indicates the strong
383 reduction effect of microstructured surface on indoor submicron particle concentration. For
384 deposition of micron particles, the particle concentration in the patterned room was 1.24 times
385 that in the control room after 1 hour's deposition, and was 178 times that in the control room
386 after deposition for 24 hours, which suggests that the microstructured surfaces have a strong
387 adverse effect on micron particle deposition, and the general impression that deposition loss
388 increases with roughness does not apply. It should be noted that in this comparison, an ideal
389 case with particle deposition as the only effect in the mass-balance equation was considered,
390 but it is enough to demonstrate the importance of taking the effect of microstructured surfaces
391 into account when calculating indoor particle concentration.
392
393 Table 1. Comparison of particle concentration in the control room and patterned room

Time	Submicron particles (0.4 μm)			Micron particles (2 μm)		
	Particle number concentration (#/m^3)		γ	Particle number concentration (#/m^3)		γ
	Control room	Patterned room		Control room	Patterned room	
T=0	2×10^{11}	2×10^{11}	1	2×10^{11}	2×10^{11}	1
T=1h	0.961 C_0	0.673 C_0	70%	0.316 C_0	0.392 C_0	1.24
T=24h	0.387 C_0	7.46e-5 C_0	0.02%	9.83e-13 C_0	1.75e-10 C_0	178

394

395 ## 4. Conclusion

396 The deposition of particles on microstructured surfaces in a chamber flow was investigated in

this study. Effects of the shape and *p/h* ratio of the microstructures were examined. The following conclusions can be drawn:

(1) An enhancement effect of the microstructured surfaces on submicron particle deposition was found, while a reduction effect was found on micron particle deposition. Both effects gradually vanished with the increasing *p/h* ratio.

(2) For submicron particles, the deposition enhancement was the strongest in triangular microstructures, followed by semi-circular convex, rectangular, and semi-circular concave microstructures respectively. On the other hand, for micron particles, the reduction of deposition did not show a significant difference among different shapes.

(3) This study provides insight into particle deposition on microstructured surfaces and contributes to indoor particle concentration control.

Acknowledgments

This work was supported by the Collaborative Research Fund (CRF) (project no. C7025-16G) and the General Research Fund (Project Nos. 16207817 & 17203220) granted by the Research Grants Council of the Hong Kong Special Administrative Region, China. The authors would like to thank Dr Hau Him Lee and Dr. Csaba HEFLER for their technical support.

References

Abadie, M., Limam, K., & Allard, F. (2001). Indoor particle pollution: Effect of wall textures on particle deposition. *Building and Environment*, *36*(7), 821–827. https://doi.org/10.1016/S0360-1323(01)00007-5

Cheng, Y. S. (1997). Wall Deposition of Radon Progeny and Particles in a Spherical Chamber. *Aerosol Science and Technology*, *27*(2), 131–146. https://doi.org/10.1080/02786829708965462

Hinds, W. C. (1999). *Aerosol technology : properties, behavior, and measurement of airborne particles.* (2nd ed), New York: Wiley, 230-245

Hussein, T., Kubincová, L., Džumbová, L., Hruška, A., Dohányosová, P., Hemerka, J., & Smolík, J. (2009). Deposition of aerosol particles on rough surfaces inside a test chamber. *Building and Environment*, *44*(10), 2056–2063. https://doi.org/10.1016/j.buildenv.2009.02.009

Hussein, T., Smolik, J., Kerminen, V. M., & Kulmala, M. (2012). Modeling dry deposition of aerosol particles onto rough surfaces. *Aerosol Science and Technology*, *46*(1), 44–59. https://doi.org/10.1080/02786826.2011.605814

Jones, A. P. (1999). Indoor air quality and health. *Atmospheric Environment*, *33*(28), 4535–4564.

Lai, A. C. K. (2002). Particle deposition indoors: A review. *Indoor Air*, *12*(4), 211–214. https://doi.org/10.1046/j.0905-6947.2002.1r159a.x

Lai, A. C. K., Byrne, M. A., & Goddard, A. J. H. (1999). Measured deposition of aerosol particles on a two-dimensional ribbed surface in a turbulent duct flow. *Journal of Aerosol Science*, *30*(9), 1201–1214. https://doi.org/10.1016/S0021-8502(99)00021-X

Lai, A. C. K., & Nazaroff, W. W. (2005). Supermicron particle deposition from turbulent

chamber flow onto smooth and rough vertical surfaces. *Atmospheric Environment*, *39*(27), 4893–4900.

Lai, A. C. K., Byrne, M. A., & Goddard, A. J. H. (2001). Aerosol deposition in turbulent channel flow on a regular array of three-dimensional roughness elements. *Journal of Aerosol Science*, *32*(1), 121–137. https://doi.org/10.1016/S0021-8502(00)00051-3

Lai, A. C. K., Byrne, M. A., & Goddard, A. J. H. (2002). Particle deposition in ventilation duct onto three-dimensional roughness elements. *Building and Environment*, *37*(10), 939–945. https://doi.org/10.1016/S0360-1323(01)00092-0

Lai, A. C. K., Wang, K., & Chen, F. Z. (2008). Experimental and numerical study on particle distribution in a two-zone chamber. *Atmospheric Environment*, *42*(8), 1717–1726. https://doi.org/10.1016/j.atmosenv.2007.11.030

Lai, A. C. K. (2006). Particle deposition and decay in a chamber and the implications to exposure assessment. *Water, Air, and Soil Pollution*, *175*(1–4), 323–334. https://doi.org/10.1007/s11270-006-9141-y

Lee, S. C., Li, W.-M., & Ao, C.-H. (2002). Investigation of indoor air quality at residential homes in Hong Kong—case study. *Atmospheric Environment*, *36*(2), 225–237.

Li, A., Ahmadi, G., Bayer, R. G., & Gaynes, M. A. (1994). Aerosol particle deposition in an obstructed turbulent duct flow. *Journal of Aerosol Science*, *25*(1), 91–112. https://doi.org/10.1016/0021-8502(94)90184-8

Lu, H., & Lu, L. (2015a). A numerical study of particle deposition in ribbed duct flow with different rib shapes. *Building and Environment*, *94*, 43–53.

https://doi.org/10.1016/j.buildenv.2015.07.030

Lu, H., & Lu, L. (2015b). Effects of rib spacing and height on particle deposition in ribbed duct air flows. *Building and Environment*, *92*, 317–327. https://doi.org/10.1016/j.buildenv.2015.04.035

Lu, H., & Lu, L. (2015c). Numerical investigation on particle deposition enhancement in duct air flow by ribbed wall. *Building and Environment*, *85*, 61–72. https://doi.org/10.1016/j.buildenv.2014.11.031

Lu, H., & Lu, L. (2016). CFD investigation on particle deposition in aligned and staggered ribbed duct air flows. *Applied Thermal Engineering*, *93*, 697–706. https://doi.org/10.1016/j.applthermaleng.2015.10.030

Lu, H., & Lu, L. (2017). Investigation of particle deposition efficiency enhancement in turbulent duct air flow by surface ribs with hybrid-size ribs. *Indoor and Built Environment*, *26*(5), 608–620. https://doi.org/10.1177/1420326X16662509

Pope, C. A., Dockery, D. W., Spengler, J. D., & Raizenne, M. E. (1991). Respiratory Health and PM 10 Pollution: A Daily Time Series Analysis . *American Review of Respiratory Disease*, *144*, 668–674. https://doi.org/10.1164/ajrccm/144.3_pt_1.668

Rashidi, S., Esfahani, J. A., & Ellahi, R. (2017). Convective heat transfer and particle motion in an obstructed duct with two side by side obstacles by means of DPM model. *Applied Sciences*, *7*(4), 431. https://doi.org/10.3390/app7040431

Shimada, M., Okuyama, K., Kousaka, Y., & Ohshima, K. (1987). Turbulent And Brownian Diffusive Deposition Of Aerosol Particles Onto A Rough Wall. *Journal of Chemical*

Engineering of Japan, *20*(1), 57–64. https://doi.org/10.1252/jcej.20.57

Thatcher, T. L., & Nazaroff, W. W. (1997). Effect of small-scale obstructions and surface textures on particle deposition from natural convection flow. *Aerosol Science and Technology*, *27*(6), 709–725. https://doi.org/10.1080/02786829708965506

Thatcher, T. L., Fairchild, W. A., & Nazaroff, W. W. (1996). Particle deposition from natural convection enclosure flow onto smooth surfaces. *Aerosol Science and Technology*, *25*(4), 359–374. https://doi.org/10.1080/02786829608965402

Thatcher, Tracy L., Lai, A. C. K., Moreno-Jackson, R., Sextro, R. G., & Nazaroff, W. W. (2002). Effects of room furnishings and air speed on particle deposition rates indoors. *Atmospheric Environment*, *36*(11), 1811–1819. https://doi.org/10.1016/S1352-2310(02)00157-7

Usui, S., Ito, K., & Kato, K. (2004). The Effect of Semi-Circular Micro Riblets on the Deposition of Diesel Exhaust Particulate. *Proceedings of 2004 SAE World Congress Detroit, Michigan*, No.2004-1-0969. https://doi.org/10.4271/2004-01-0969

Wan, M.-P., Wu, C.-L., SzeTo, G.-N., Chan, T.-C., & Chao, C. Y. H. (2011). Ultrafine particles, and PM2. 5 generated from cooking in homes. *Atmospheric Environment*, *45*(34), 6141–6148.

Wang, Y., Fan, X., Li, A., Shang, L., & Wang, H. (2018). Deposition of fine particles on vertical textile surfaces: A small-scale chamber study. *Building and Environment*, *135*, 308–317. https://doi.org/10.1016/j.buildenv.2018.03.003

Xu, H., Fu, S. C., Chan, K. C., & Chao, C. Y. H. (2020). Investigation of particle deposition

on a micropatterned surface as an energy-efficient air cleaning technique in ventilation ducting systems. *Aerosol Science and Technology*, *54*(10), 1210–1222. https://doi.org/10.1080/02786826.2020.1767758

Xu, H., Fu, S. C., Chan, K. C., Qiu, H., & Chao, C. Y. H. (2020). Bio-inspired patterned surface for submicron particle deposition in a fully developed turbulent duct. *Building Simulation*, *13*(5), 1111–1123. https://doi.org/10.1007/s12273-020-0681-7

Xu, H., Fu, S. C., Leung, W. T., Lai, T. W., & Chao, C. Y. H. (2020). Enhancement of submicron particle deposition on a semi-circular surface in turbulent flow. *Indoor and Built Environment*, *29(1),* 101–116. https://doi.org/10.1177/1420326X19853862

Xu, M., Nematollahi, M., Sextro, R. G., Gadgil, A. J., & Nazaroff, W. W. (1994). Deposition of tobacco smoke particles in a low ventilation room. *Aerosol Science and Technology*, *20*(2), 194–206. https://doi.org/10.1080/02786829408959676

Yu, K. P., Shih, H. C., Chen, Y. C., & Yang, X. E. (2017). Effect of turbulence intensity and particle characteristics on the deposition of submicron particles enhanced by the ionic air purifier. *Building and Environment*, *114*, 166–177. https://doi.org/10.1016/j.buildenv.2016.12.023